JOC The Journal of Organic Chemistry

Article

pubs.acs.org/joc

A DFT-Based Analysis of the Gold-Catalyzed Cycloisomerization of 1-Siloxy 1,5-Enynes to Cyclohexadienes

Elena Soriano* and José Marco-Contelles

Instituto de Química Orgánica General (CSIC), Juan de la Cierva, 3, 28006-Madrid, Spain

Supporting Information

ABSTRACT: In this work, we present a deep theoretical study on the intriguing and unexpected gold-catalyzed cycloisomerization of siloxy enynes to cyclohexadienes. To this end, we have evaluated the electronic and steric properties for three types of alkynyl substituents along the reaction paths and the implications on the evolution through divergent, competitive pathways. For an alkynyl −OR substituent, the results strongly suggest a polarization of the π electrons along the delocalized C2−C1−O system in the key cyclopropyl−carbene intermediate, which is enhanced by the bulkiness of the R group. The results reproduce the experimental observations in excellent agreement and provide interesting and useful clues for predicting the effects of the alkynyl substituent on the nature of the key intermediate and, hence, on the reactivity mode and selectivity.

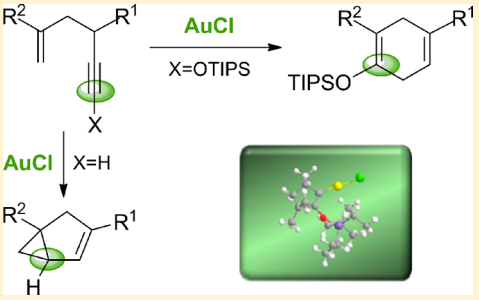

1. INTRODUCTION

Platinum- and gold-catalyzed cycloisomerizations of polyunsaturated precursors provide rapid and efficient access to a variety of cyclic structural motifs[1] for a wide range of synthetic applications.[2] Within this rapidly developing area of catalysis involving metal complexes as carbophilic π acids, enyne cycloisomerizations have been particularly well-studied.[3] In this context, cycloisomerizations of 1,5-enynes[4] and 1,6-enynes[5] were found to produce a great diversity of products via diverse reaction cascades. Accordingly, a variety of noble-metal-catalyzed reactions involving 1,*n*-enynes that bear a protected hydroxyl group at different positions have been investigated.[6] These transformations are highly dependent on the molecular structure of the enyne, and subtle variations of the substituents result in a divergent reactivity.

Thus, it has been reported that 1,6-enynes substituted with alcohols, ethers, and silyl ethers at the propargylic position undergo stereoselective transformations through a mechanism involving intramolecular 1,5-migration of OR groups, leading to bi- or tricyclic products.[7] Reactions involving 1,*n*-enynes that bear a protected hydroxyl group at the 3-position are rare,[8] although results of employing 3-silyloxy 1,5-enynes[9] and 3-methoxy 1,6-enynes[10] have been also reported. In the same vein, it has been communicated by Kozmin and co-workers the Au-catalyzed skeletal reorganization of 1-siloxy-5-en-1-ynes to furnish unexpected highly substituted siloxycyclohexadienes, such as **1** (Scheme 1), which, upon protodesilylation of the resulting cyclohexadienes **2**, can afford conjugated and/or nonconjugated enones, highlighting the general synthetic utility of this catalytic process. Introduction of the quaternary center at the C3 (for numbering, see Chart 1) position of the enyne (**3**) resulted in exclusive formation of 1,3-cyclohexadienes (**4**) (Scheme 1).

Scheme 1. Gold-Mediated Cycloisomerization of 1-Siloxy-5-en-1-ynes[11]

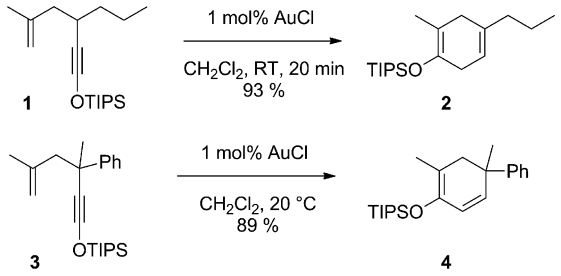

Chart 1. Structure of the 1,5-Enynes Investigated in This Work

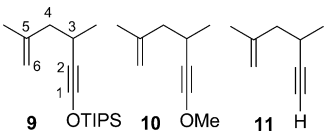

Both alkyl and aryl substitution at the C3 position were well-tolerated. These results reveal a different reactivity than that observed for unprotected reactants, which generally leads to products with a bicyclo[3.1.0]hexene skeleton through the initial cylopropanation via *endo*-dig cyclization, and a strong and intriguing effect of the alkynyl substituent on this unusual reactivity.

During this process, the siloxy group formally migrates from the C1 to the C6 position. To justify these results, the authors

Received: May 22, 2012
Published: June 25, 2012

dx.doi.org/10.1021/jo301057j | J. Org. Chem. 2012, 77, 6231−6238

proposed a mechanism involving a series of 1,2-alkyl shifts (Scheme 2). Activation of siloxy alkyne (**A**) with AuCl toward

Scheme 2. Proposed Mechanism by Kozmin and Co-Workers for the Au-Catalyzed Cycloisomerization of 1-Silyloxy 1,5-enynes[11]

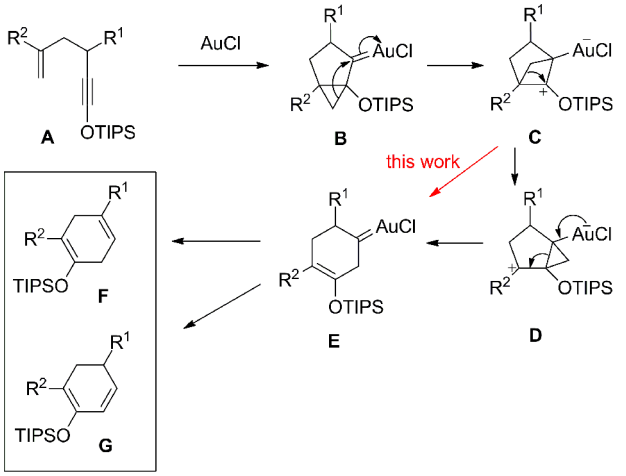

the intramolecular attack by the alkene would result in the cyclization to give cyclopropyl gold carbene **B**, which could undergo a highly unusual 1,2-alkyl shift to give oxocarbenium ion **C**. Another 1,2-alkyl shift, followed by fragmentation of the zwitterionic intermediate **D**, affords six-membered gold carbene **E**. Depending on the nature of the R^1 and R^2 substituents of the enyne, gold carbene **E** can participate in two alternative elimination pathways to afford isomeric 1,3- and 1,4-cyclohexadienes (**F** and **G**) with a concomitant regeneration of AuCl.

Later on, these authors have expanded the scope of this process and have reported the formation of a broad range of 1,3-cyclohexadienes from enynes bearing terminal, internal, and arene-conjugated alkynes.[11b]

Although the basic mechanistic pathways for homogeneous gold-catalyzed cycloisomerizations are better understood nowadays, numerous questions still remain unanswered concerning, for instance, the nature of the intermediate species or the factors favoring one pathway over another. Herein, we present a theoretical study[12] on these two intriguing cycloisomerizations of 1,5-enynes[13] to get insight into the key role played by the silyloxy group and into the divergent pathways that it promotes.

2. RESULTS AND DISCUSSION

2.1. Reaction Pathways. Kozmin and co-workers suggested that the divergent formation of the dienes in the AuCl-catalyzed reaction might be due to the presence of a siloxy group at the alkyne terminus, which would strongly favor the formation of dienes because of the efficient stabilization of cationic intermediate **C** (Scheme 2).[11] In this context, we wonder if other stabilizing substituents at the alkyne could also promote the same path.

To this end, we have chosen three structures for this study: **9**, the model system bearing the 1-silyloxy substituent; **10**, a precursor with a 1-methoxy substituent; and **11**, a simplified model lacking a substituent at the alkyne moiety (Chart 1). We present the study of the mechanism of cycloisomerization of **9**, and then we compare the energy profile with that for the usual formation of [3.1.0]bicycloalkenes. Additionally, we compare the two pathways for the models to get insight into the effect of the substituent.

The computations for the cyclization of **9** and **10** indicated that the coordination of the enyne to AuCl involves a larger elongation of the triple bond (1.251 and 1.250 Å) than that of **11** (1.239 Å, Figure 1) since the uncomplexed alkyne showed similar CC bond lengths (1.208−1.210 Å). Analogously, while the C1−Au bond (2.179 Å) (for numbering, see Chart 1) is shorter than C2−Au (2.302 Å) for **11**-[Au], the opposite trend is observed for **9**-AuCl (2.409 and 2.153 Å) and **10**-[Au] (2.442 and 2.147 Å) that is accompanied by a shortening of the typical Csp−O bond (1.283 Å for **10**-AuCl and 1.274 Å for **9**-AuCl).

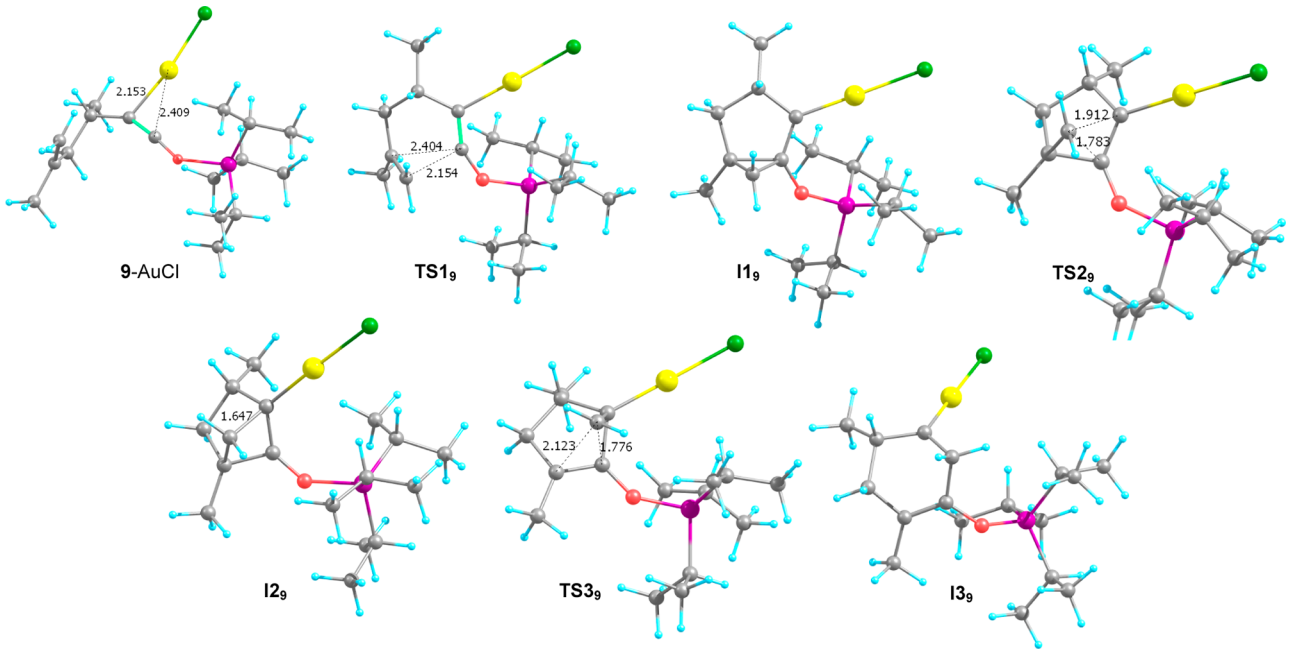

Figure 1. Optimized structures for the AuCl-catalyzed cycloisomerization of enyne **9**. Relevant distances are shown in angstroms.

dx.doi.org/10.1021/jo301057j | J. Org. Chem. 2012, 77, 6231−6238

These effects, which probably reflect the strongly donating character of the −OR substituents,[14,15] increase the electrophilicity of C1 as also is suggested by the computed NPA charges: +0.441 for C1 versus −0.316 for C2 in **9**-AuCl, +0.417/−0.285 in **10**-AuCl, and −0.326/+0.023 in **11**-AuCl.

The complexed reactant **9**-AuCl must surmount a free energy barrier of 13.0 kcal/mol through the *anti*-transition structure $\mathbf{TS1_9}$ to reach the intermediate $\mathbf{I1_9}$, which lies 6.3 kcal/mol below the initial complex (Table 1; see also Table S1 in the Supporting Information). A slightly lower barrier is computed for **10** ($\mathbf{TS1_{10}}$), probably due to the lower steric hindrance of the alkyne substituent, while the absence of the stabilizing effect of an ether moiety gives rise to a higher barrier for **11** ($\mathbf{TS1_{11}}$).

Table 1. Relative Free Energies in the Gas Phase and in Solution (Dichloromethane) (in kcal/mol, 298.15 K) Computed at the M06/6-311G(d,p)-LANL2DZ Level for the AuCl-Catalyzed Cycloisomerization of Enynes 9−11

	11		10		9	
	ΔG	ΔG_{dis}	ΔG	ΔG_{dis}	ΔG	ΔG_{dis}
R	0.0	0.0	0.0	0.0	0.0	0.0
TS1	18.1	12.3	12.0	6.1	13.0	7.2
I1	−7.3	−11.3	−8.9	−12.6	−6.3	−9.7
TS2	16.6	5.3	−1.9	−6.7	0.2	−4.5
I2	−4.1	−6.6	−2.5	−9.6	−1.4	−7.0
TS3			5.6	−1.7	7.4	0.0
I3			−7.4	−9.6	−5.1	−8.0
TS4(H3)	−0.3	−5.2	−2.2	−7.5	3.4	0.4
P(H3)	−38.0	−36.8	−40.3	−39.7	−34.8	−36.2
TS4(H6)	2.6	−4.1	2.8	−2.9	7.5	4.2
P(H6)	−34.0	−34.2	−36.0	−36.0	−32.7	−34.0
$\mathbf{TS_{bicycl}}$	7.8	2.4	6.6	1.1	11.5	6.1
$\mathbf{P_{bicycl}}$	−29.9	−28.6	−30.7	−30.7	−24.7	−23.5

At this point, and probably as a result of the bulky OTIPS moiety, the C1−C6 bond (1.593 Å) is larger and the C6−C2 is shorter (2.491 Å) in $\mathbf{I1_9}$ than in $\mathbf{I1_{10}}$ (1.567 and 2.551 Å) and $\mathbf{I1_{11}}$ (1.568 and 2.548 Å) (Figure 1; for numbering, see Chart 1). This effect favors the 1,2-alkyl shift to give oxocarbenium species $\mathbf{I2_9}$, as suggested by the calculations that reveal a slightly lower barrier from the intermediate $\mathbf{I1_9}$ (6.5 kcal/mol) than from $\mathbf{I1_{10}}$ (7.0 kcal/mol).

In the transition structure $\mathbf{TS2_9}$, the breaking C1−C6 bond is 1.783 Å, whereas the incipient C2−C6 is developing (1.912 Å). A slightly later transition structure is observed for **10** ($\mathbf{TS2_{10}}$) (1.788 and 1.890 Å). This step is endothermic for both structures due to the ring tension of the oxocarbenium intermediate $\mathbf{I2_{9(10)}}$ (**C**, Scheme 2).

Obviously, this kind of intermediate is not feasible for **11**; instead, we have located a considerably less stable transition-state structure $\mathbf{TS2_{11}}$ (16.6 kcal/mol above **11**-AuCl) where C6 is nearly symmetrically bonded to C1 (1.621 Å) and C2 (1.631 Å) while the bond with C5 is breaking (1.804 Å). IRC calculations confirm that this transition structure comes from the carbene intermediate $\mathbf{I1_{11}}$ and evolves to the gold carbene intermediate of type **E** (Scheme 2; $\mathbf{I3_{11}}$, Figure 3).

On the other hand, $\mathbf{I2_9}$ leads to the carbene of type **E** (Scheme 2; $\mathbf{I3_9}$ in Figure 2) through a transition structure $\mathbf{TS3_9}$ showing a broken C5−C6 bond (2.123 Å) and developed C1−C6 bond (1.776 Å), whereas the C2−C6 bond is shortened (1.490 Å). For $\mathbf{TS3_{10}}$, similar values are observed (2.128, 1.771, and 1.490 Å), highlighting the effect of an ether group on the evolution of these catalyzed cycloisomerization processes. This insertion step is exothermic and proceeds with a low free energy barrier (Table 1). Note that the calculations ruled out the formation of structure **D** (Scheme 2) as an effective intermediate along the reaction pathway, as was proposed by Kozmin and co-workers.[11]

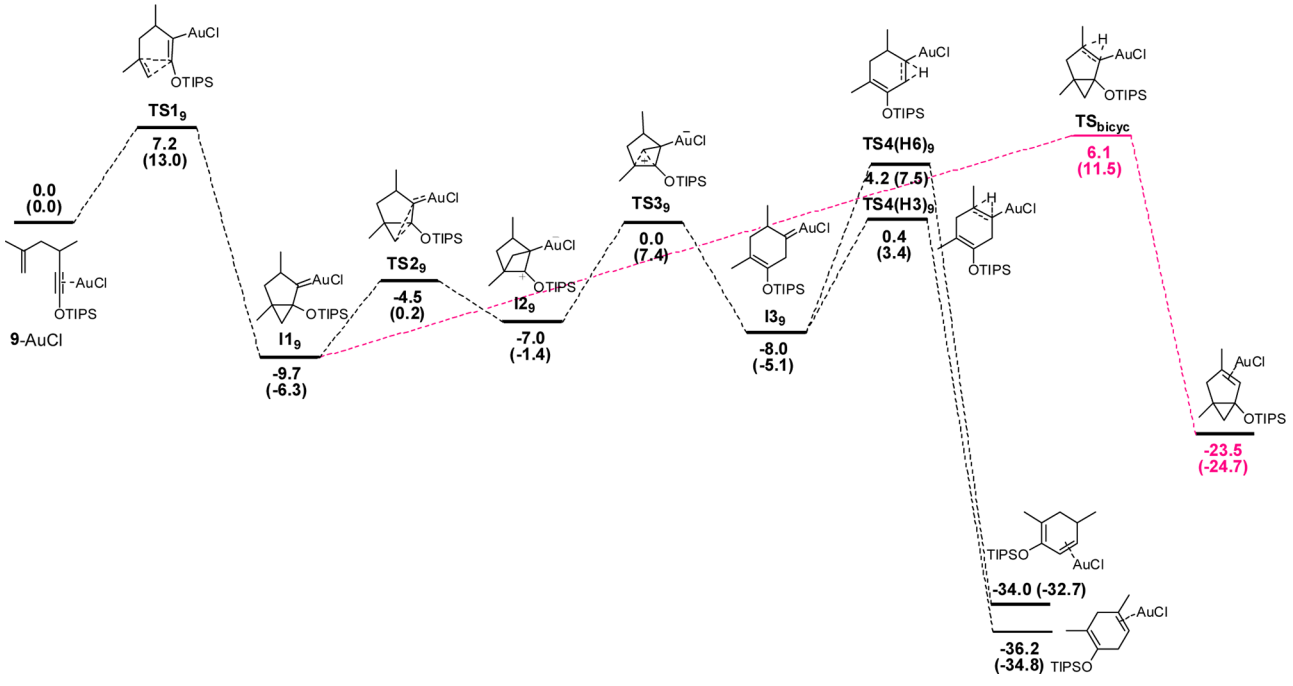

Figure 2. Calculated free energy profiles in solution (dichloromethane) (in kcal/mol) for the gold-catalyzed cycloisomerization of **9** to dienes (black) and to bicyclo[3.1.0]hexanes (pink). Free energy values in the gas phase are shown in parentheses.

dx.doi.org/10.1021/jo301057j | J. Org. Chem. 2012, 77, 6231−6238

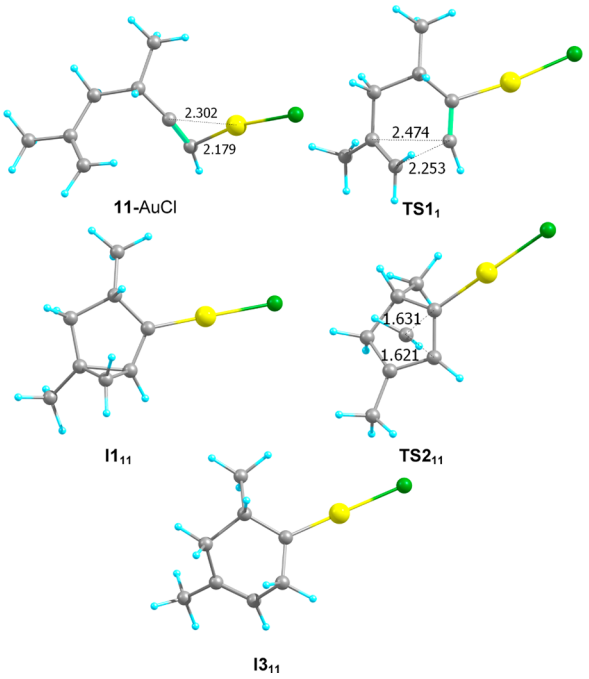

Figure 3. Optimized structures for the AuCl-catalyzed cycloisomerization of enyne **11**. Relevant distances are shown in angstroms.

Finally, two paths for the [1,2]-H shift can be envisaged that result in the formation of 1,3- and 1,4-dienes (Figure 4). For

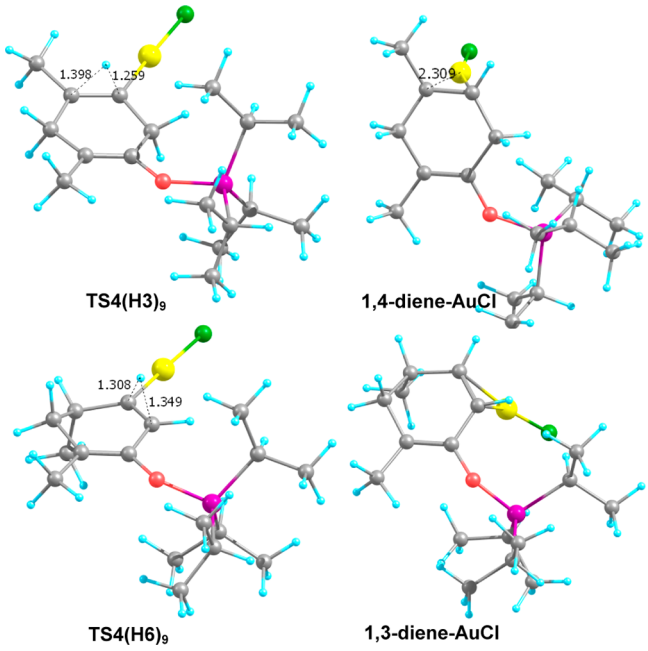

Figure 4. Optimized structures for the competing [1,2]-H shifts in the AuCl-catalyzed cycloisomerization of enyne **9**. Relevant distances are shown in angstroms.

the three model systems, the [1,2]-H shift from C3 leading to 1,4-dienes (**F**) is kinetically more favorable (by about 4 kcal/mol) than from C6 to 1,3-dienes (**G**), which fully agrees with the experimental observations. This preference is probably due to the stabilizing effect of the alkyl substituent at C3, as the computed NPA charges point out in **TS4(H3)$_9$** (charge at C3(CH_3) = +0.227) and **TS4(H6)$_9$** (charge at C6(H) = +0.033).

To complete the analysis of the divergent mechanism offered by the 1-siloxy-5-en-1-ynes in the AuCl-catalyzed reorganization, we have also explored the alternative [1,2]-H shift from **I1$_9$**, which would lead to the well-known formation of [3.1.0]bicyclohexenes[4a,d,16] through the transition structure **TS$_{bicyc}$** (see Figure S1 in the Supporting Information). According to our computations of the free energy profiles, only the system **11** should follow preferentially this path. In contrast, the more favorable pathway computed for **9** is the formation of the 1,4-diene. For **10**, the step leading to the [3.1.0]bicyclohexene framework shows a barrier of 6.6 kcal/mol, only 1.0 kcal/mol higher than that for the 1,2-alkyl shift to the formation of the second carbene **I3$_{10}$**, suggesting the bulkiness requirement of the alkynyl substituent to preferentially drive the reaction to the formation of the 1,4-diene.

2.2. Solvent Effects. Table 1 and Figure 2 summarize the reaction profiles computed in the gas phase and in solution (dichloromethane) and show the effect of solvation on the barriers within each path and in the competition between mechanisms. The solvent stabilizes the intermediates and transition-state structures, mainly due to the electrostatic terms. However, this stabilization is stronger for the third step, that is, the insertion step, the fragmentation of the intermediate **I2$_9$** (Table 1) with concomitant methylene insertion to afford the six-membered ring intermediate **I3$_9$**. This is not an unexpected result since **I2$_9$** and the following **TS3$_9$** show a zwitterionic character (see Figure S2 in the Supporting Information) and the highest dipole moment (11.3 and 12.2 D, respectively) of the structures involved along the path (between 7.4 and 11.1 D).

From the results, we can conclude that, although each profile is stabilized upon solvation, the solvent effects enhance the selectivity and preference for one mechanism over another for the three model systems. In fact, **TS3$_9$** is more stabilized by solvation (7.4 kcal/mol) than **TS$_{bicyc}$** to form the bicycle[3.1.0]-hexene (by 5.4 kcal/mol). The overall process is highly exergonic and, therefore, fundamentally irreversible ($\Delta G_{298.15\ K}$ = −36.2 kcal/mol).

2.3. Structure, Bonding, and Properties of the Intermediate Structures. To get further insights into the mechanism, we have analyzed the intermediate species,[17] in particular, the carbenoid structures, and the effect of the alkynyl substituent on the reaction evolution.

The nature of bonding in the carbenoids intermediates remains unclear and is still the material of intense debate.[18] The discussion focuses on the extent of carbene character versus gold-stabilized carbocation character in these intermediates. Fürstner has suggested that Au(I) carbene intermediates in cycloisomerizations of enynes are more consistently described as gold-stabilized carbocations,[19a] which might lack significant π-back-bonding due to a mismatch in orbital size.[19b] Subsequently, in an experimental and theoretical study, Toste and Goddard argued that the character of these intermediates lies on a continuum ranging from metal-stabilized singlet carbenes to metal-coordinated carbocations, which is determined by both the substitution and the ancillary ligand of gold.[20]

Figure S3 (see the Supporting Information) shows the evolution of the Au−C2 distance along the reaction. The distance values suggest single rather higher bond character for all, but for **I1$_9$** and **I3$_9$**, which present values of 1.972 and

dx.doi.org/10.1021/jo301057j | J. Org. Chem. 2012, 77, 6231−6238

1.968.[21,22] Because of their relevance on the evolution, these two structures merit a deeper study to shed light on the current gold-stabilized carbocations/gold carbene character.

In contrast to the case for many other transition metals, gold in its +1 oxidation state maintains a nearly closed 5d shell and only one vacant valence orbital (6s), as our NBO analyses reveal (see Tables S2−S4 in the Supporting Information). This analysis finds that the gold 5d and 6s orbitals dominate its bonding, with negligible participation of the gold 6p orbital. Similar observations have been made by other authors.[23] As a result, a model of a four-electron−three-center bond has been proposed, in which the gold atom, the ligand moiety, and the carbon atom C2 unit participate. Additionally, it has been established that the metal center is able to form two π bonds by donation from perpendicular filled d orbitals into empty π acceptors on the ligand and C2. Although these two bonds are not mutually exclusive, they compete for electron density from gold. Therefore, because the π-donating ligand Cl should increase back-donation to gold, and then gold to C2 by π-donation, a very short gold−carbon bond can be formed (as for $\mathbf{I1_9}$ and $\mathbf{I3_9}$), as the bond distances and NBO analysis suggest.

The computed Wiberg bond orders for the Au−C2 bond show the highest values for these two species, 0.76 and 0.81 for $\mathbf{I1_9}$ and $\mathbf{I3_9}$, respectively (Table S2 in the Supporting Information). These values exceed the maximum value of 0.5 for a σ bond.

Thus, on the basis of NBO analysis, we find that the Au−C2 bond for $\mathbf{I1_9}$ and $\mathbf{I3_9}$ is composed of weak σ (23%) and π components (77%). The σ interaction originates from the C2 sp^2 lone pair partially overlapping the 6s orbital on gold, which is partially populated by donation from the Cl ligand. In addition, the π component of the bond is a highly polarized dπ-to-pπ donation from an Au lone pair to the empty pπ orbital on C2, showing an interaction of 27.0 and 30.5 kcal/mol, for $\mathbf{I1_9}$ and $\mathbf{I3_9}$, respectively.[20] Therefore, a non-negligible fraction of the electron density is transferred from gold to the organic fragment via π-back-donation. These data confirm previous discussions on the topic of the character of gold-carbenoids, suggesting that the orbital size mismatch does not appear to be large enough to suppress the π-back-bonding interaction.[24] More important for our current study, the structural and bonding analyses suggest that the intermediates $\mathbf{I1_9}$ and $\mathbf{I3_9}$ exhibit a high character of a gold−carbene bond.

Regarding the effect of the silyl ether, the C1−O bond distances computed for **9** and **10** indicate a parallel evolution along the path, although they are slightly shorter for **9**. Thus, the C1−O bond distance is gradually shortening from 1.357 Å in $\mathbf{I1_9}$ to 1.305 Å in $\mathbf{TS2_9}$ and 1.274 Å in $\mathbf{I2_9}$, in accord with the formation of an oxocarbenium-type intermediate (Figure 5).

This variation is also supported by the calculated Wiberg C1−O bond order, the minimum at $\mathbf{I1_9}$ and the maximum at $\mathbf{I2_9}$, with a value of 1.29 (Figure 5). The computed NPA charge at the O atom also follows this trend, that is, a reduction of charge Δ(charge) = +0.14e in going from $\mathbf{I1_9}$ to $\mathbf{I2_9}$, which is transferred to C1 by pπ-to-pπ donation from the O lone pair to the new empty pπ orbital on C1. These results suggest a strong stabilization of the zwitterionic structure $\mathbf{I2_9}$ by the ether moiety. Moreover, these effects are slightly lower for **10** (Δ(charge) = +0.09e)), which implies a somewhat weaker stabilizing effect of an alkyl ether, in good agreement with the computed free-energy profile.

As discussed above, the π-donating ligand Cl increases back-donation to gold, and then gold to C2 by π-donation. However,

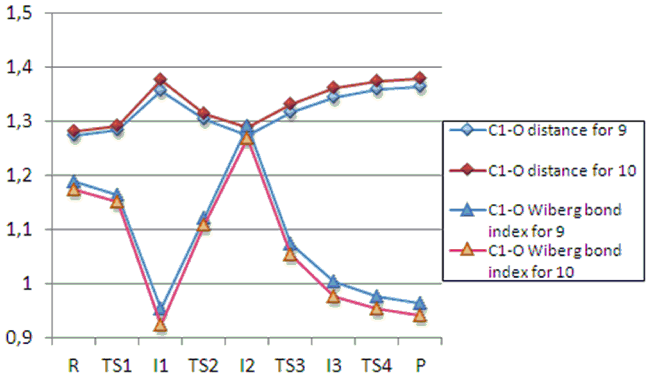

Figure 5. Evolution of the C1−O bond distance (in Å) and the Wiberg bond order along the AuCl-catalyzed cycloisomerization of **9** and **10**. The results suggest strong charge transference from the O lone pair to C1 for the structure **I2**.

this donation is less effective for $\mathbf{I1_9}$ than for $\mathbf{I1_{11}}$, as orbital analysis and distances indicate (Au−Cl/Au−C2: 2.353/1.972 Å for $\mathbf{I1_9}$, 2.347/1.963 Å for $\mathbf{I1_{11}}$). This effect is due to repulsive steric interactions between the bulky substituent and the catalyst, since the system **10** shows similar values to the unsubstituted system (2.347/1.965 Å for $\mathbf{I1_{10}}$). Moreover, the C1−C2 distance is lower in $\mathbf{I1_9}$ (1.422 Å) than in $\mathbf{I1_{10}}$ (1.427 Å) and $\mathbf{I1_{11}}$ (1.428 Å). These accumulated data strongly point out a polarization of the π electrons along the delocalized C2−C1−O system in $\mathbf{I1_9}$ enhanced by the bulkiness of the TIPS group.

2.4. Reactivity and Selectivity. To assess the factors that might lead to a preference for the 1,2-alkyl shift over the well-known 1,2-H shift, we have compared the electronic, geometric, and thermodynamic data of the common key intermediate **I1** for both processes for the three model systems.

A close geometric comparison reveals some differences. The cyclopropane C1−C6 bond length is 1.568, 1.567, and 1.593 Å, for $\mathbf{I1_{11}}$, $\mathbf{I1_{10}}$, and $\mathbf{I1_9}$, respectively. Therefore, a bulky moiety, as a TIPSO group, promotes an elongation of the C1−C6 bond in the carbene structure $\mathbf{I1_9}$, which would evolve to $\mathbf{I2_9}$ to alleviate the steric demand by the silyl ether in a step assisted by the stabilization just provided by the silyl ether moiety. Additionally, the values for the cyclopropane C1−C5 bond are 1.582, 1.603, and 1.609 Å, for $\mathbf{I1_{11}}$, $\mathbf{I1_{10}}$, and $\mathbf{I1_9}$, respectively. Finally, the shortening of the C1−C2 bond for $\mathbf{I1_9}$ (1.422 Å) as compared with $\mathbf{I1_{10}}$ (1.427 Å) and $\mathbf{I1_{11}}$ (1.428 Å), is remarkable.

The NBO analysis for $\mathbf{I1_9}$ indicates a partial overlap of the O lone pair and the empty π orbital of the C1−C2, the π orbital of the C1−C6, and the π orbital of the C1−C5. These interactions could account for the former structural results. In $\mathbf{TS2_9}$, only the first interaction is relevant and increased. More importantly, the breaking C1−C6 bond electron pair partially migrates as a C6 lone pair, forming in $\mathbf{TS2_9}$ an occupied pπ orbital (82% of π character) that strongly overlaps with the empty pπ orbital at C2 (94% of π character).[25] The density from the C2 lone pair is shifted toward the p orbital at C1, contributing to the developing pπ C1−O in the subsequent $\mathbf{I2_9}$. These strong interactions stabilize the transition structure $\mathbf{TS2_9}$, even though there exists the high ring tension of the forming cycloadduct $\mathbf{I2_9}$. These interactions are lower for the system **10**, in agreement with the computed lower step barrier (6.5 kcal/mol for $\mathbf{TS2_9}$ vs 7.0 kcal/mol for $\mathbf{TS2_{10}}$).

dx.doi.org/10.1021/jo301057j | J. Org. Chem. 2012, 77, 6231−6238

Thus, as suggested above, a polarization of the π electrons along the delocalized C2−C1−O system in $\mathbf{I1_9}$ is enhanced by the bulkiness of the alkynyl substituent, promoting the pathway toward the formation of $\mathbf{I2_9}$.

The insertion step via $\mathbf{TS3_9}$ completes the 1,2-alkyl shift in a exothermic step because of the released steric tension. C6 migrates with the partial C5−C6 electron pair, which, at the transition structure ($\mathbf{TS3_9}$), forms an occupied forming π orbital (88% of π character in $\mathbf{TS3_9}$) that overlaps with the new empty pπ orbital at C1 (88% at C1), favoring the formation of the new C1−C5 double bond in $\mathbf{I3_9}$.

On the other hand, the 1,2-H shift takes place from **I1** with a barrier of 15.1 kcal/mol for the unsubstituted system **11**, similar to **10** (15.5 kcal/mol), but lower than for **9**, 17.8 kcal/mol. These results could be ascribed to the electronic effects at C2 and steric effects from the alkynyl substituent described above. The 1,2-H shift is affected by the increased population of the C2 pπ orbital.[26] The bulky OTIPS group generates steric repulsion with the AuCl unit in $\mathbf{I1_9}$, as the Au−C2−C1 bond angle value suggests for the three systems: 124.4° for $\mathbf{I1_{11}}$, 124.8° for $\mathbf{I1_{10}}$, and 127.5° for $\mathbf{I1_9}$. According to our analysis, this geometric distortion increases the population at C2 for **9**, as the NPA charges at C2 reveal (−0.078 and −0.008 for $\mathbf{I1_9}$ and $\mathbf{I1_{11}}$, respectively), thus suggesting that the Au dπ electrons have more overlap with the C pπ orbital. The study reveals a population of the C2 pπ orbital that increases by donation from the Au dπ electrons in the order of **11** < **10** < **9**.[27]

In summary, these results highlight the crucial role of the alkynyl substituent, and, in particular, the siloxy alkyne moiety, in the outcome of the enyne cycloisomerization. The key intermediate can follow two routes: the formation of the 1,3-dienes (and/or 1,4-dienes) and the alternative formation of the bicyclo[3.1.0]hexane skeleton. The selectivity for either pathway arises from a preference governed by electronic properties and steric effects from the alkynyl substituent in the gold-stabilized cyclopropyl−carbene intermediate. Thus, while a OTIPS substituent favors the first pathway, a less bulky ether results in a loss of efficiency for this process, only 1 kcal/mol kinetically more favorable than the formation of the pertinent bicyclo[3.1.0]hexene.

3. CONCLUSIONS

Herein, we present a deep theoretical study on the intriguing cycloisomerization reported by Kozmin and co-workers.[11] The Au-catalyzed cycloisomerization of siloxy enynes provides access to 1,2- and 1,3-cyclohexenones. The current study provides insight into the key role played by the alkynyl substituent into the divergent pathways that it promotes. For an alkynyl −OR substituent, the results strongly suggest a polarization of the π electrons along the delocalized C2−C1−O system in the key cyclopropyl−carbene intermediate, which is enhanced by the bulkiness of the R group, that promotes the pathway toward the formation of the cyclohexadiene. Moreover, our calculations confirm that the 1,2-H shift from the key intermediate to the formation of the well-known [3.1.0]bicyclohexene is affected by increased population of the C2 pπ orbital by donation from the Au dπ electrons. Thus, the selectivity for either pathway arises from a preference governed by electronic properties and steric effects from the alkynyl substituent in the gold-stabilized cyclopropyl−carbene intermediate.

To sum up, our results provide useful insights into the effects of the alkynyl substituent on the gold-stabilized carbocations/gold carbene character of the key intermediate and, hence, on the reactivity mode and selectivity of the catalyzed transformation.

4. COMPUTATIONAL METHODS

The calculations have been performed using the Gaussian 03[28] and Gaussian 09[29] packages. Geometry optimizations were carried out at DFT in its Kohn−Sham approach, with the B3LYP functionals,[30] and a 6-31G(d,p) basis set for the main group atoms and the LANL2DZ electron core potential[31] and associated basis set for gold. The stationary points thus obtained were characterized by means of harmonic analysis, and for all the transition structures, the normal mode related to the imaginary frequency corresponds to the nuclear motion along the reaction coordinate under study. In several significant cases, intrinsic reaction coordinate (IRC)[32] calculations were performed to unambiguously connect transition structures with reactants and products. To get more precise results, we have applied the functional developed by Truhlar et al., M06,[33] configured for a better description of dispersive forces, and which has been described that provides better results in the study of processes catalyzed by Au.[34] These calculations have been performed with the 6-311G(d,p) basis set for nongold atoms. Solvation effects were taken into consideration with the polarizable continuum model (PCM)[35] and the molecular cavity created with the UAKS radii set.

■ ASSOCIATED CONTENT

Ⓢ Supporting Information

Additional results for plausible paths, thermodynamic data, electronic computations, Cartesian coordinates, SCF energies, and the number of imaginary frequencies of all structures. This material is available free of charge via the Internet at http://pubs.acs.org.

■ AUTHOR INFORMATION

Corresponding Author

*E-mail: esoriano@iqog.csic.es.

Notes

The authors declare no competing financial interest.

■ ACKNOWLEDGMENTS

The authors thank Prof. S. Kozmin for reviewing this article. Additionally, the authors are grateful to the Centro de Supercomputación de Galicia (CESGA) for the generous allocation of computing resources. E.S. thanks MICINN for grant CTQ2009-10478.

■ REFERENCES

(1) For recent reviews, see: (a) Hashmi, A. S. K. *Chem. Rev.* **2007**, *107*, 3180. (b) Jimenez-Núñez, E.; Echavarren, A. M. *Chem. Rev.* **2008**, *108*, 3326. (c) Fürstner, A.; Davies, P. W. *Angew. Chem., Int. Ed.* **2007**, *46*, 3410. (d) Skouta, R.; Li, C.-J. *Tetrahedron* **2008**, *64*, 4917. (e) Gorin, D. J.; Toste, F. D. *Nature* **2007**, *446*, 395. (f) Hashmi, A. S. K.; Hutchings, G. J. *Angew. Chem., Int. Ed.* **2006**, *45*, 7896. (g) Li, Z.; Brouwer, C.; He, C. *Chem. Rev.* **2008**, *108*, 3239. (h) Arcadi, A. *Chem. Rev.* **2008**, *108*, 3266. (i) Gorin, D. J.; Sherry, B. D.; Toste, F. D. *Chem. Rev.* **2008**, *108*, 3351. (j) Sengupta, S.; Shi, X. *ChemCatChem* **2010**, *2*, 609. (k) Corma, A.; Leyva-Pérez, A.; Sabater, M. J. *Chem. Rev.* **2011**, *111*, 1657. (l) Hashmi, A. S. K.; Rudolph, M. *Chem. Commun.* **2011**, *47*, 6536.

(2) (a) Rudolph, M.; Hashmi, A. S. K. *Chem. Soc. Rev.* **2012**, *41*, 3129. (b) Fürstner, A. *Chem. Soc. Rev.* **2009**, *38*, 3208. (c) Kirsch, S. F. *Synthesis* **2008**, 3183. For selected applications in total synthesis, see: (d) Fürstner, A.; Szillat, H.; Gabor, B.; Mynott, R. *J. Am. Chem. Soc.* **1998**, *120*, 8305. (e) Trost, B. M.; Doherty, G. A. *J. Am. Chem. Soc.* **2000**, *122*, 3801. (f) Simmons, E. M.; Sarpong, R. *Org. Lett.* **2006**, *8*, 2883. (g) Fürstner, A.; Kennedy, J. W. J. *Chem.—Eur. J.* **2006**, *12*,

7398. (h) Linghu, X.; Kennedy-Smith, J. J.; Toste, F. D. *Angew. Chem., Int. Ed.* **2007**, *46*, 7671.
(3) For reviews, see: (a) Ma, S.; Yu, S.; Gu, Z. *Angew. Chem., Int. Ed.* **2006**, *45*, 200. (b) Zhang, L.; Sun, J.; Kozmin, S. A. *Adv. Synth. Catal.* **2006**, *348*, 2271. (c) Nieto-Oberhuber, C.; López, S.; Jiménez-Núñez, E.; Echavarren, A. M. *Chem.—Eur. J.* **2006**, *12*, 5916.
(4) For selected examples, see: (a) Luzung, M. R.; Markham, J. P.; Toste, F. D. *J. Am. Chem. Soc.* **2004**, *126*, 10858. (b) Zhang, L.; Kozmin, S. A. *J. Am. Chem. Soc.* **2005**, *127*, 6962. (c) Couty, S.; Meyer, C.; Cossy, J. *Angew. Chem., Int. Ed.* **2006**, *45*, 6726. (d) Mamane, V.; Gress, T.; Krause, H.; Fürstner, A. *J. Am. Chem. Soc.* **2004**, *126*, 8654.
(5) For selected examples, see inter alia: (a) Toullec, P. Y.; Genin, E.; Leseurre, L.; Genêt, J.-P.; Michelet, V. *Angew. Chem., Int. Ed.* **2006**, *45*, 7427. (b) Schelwies, M.; Dempwolff, A. L.; Rominger, F.; Helmchen, G. *Angew. Chem., Int. Ed.* **2007**, *46*, 598. (c) Nieto-Oberhuber, C.; López, S.; Muñoz, M. P.; Jiménez-Núñez, E.; Buñuel, E.; Cárdenas, D. J.; Echavarren, A. M. *Chem.—Eur. J.* **2006**, *12*, 1694.
(6) (a) Mainetti, E.; Mouriès, V.; Fensterbank, L.; Malacria, M.; Marco-Contelles, J. *Angew. Chem., Int. Ed.* **2002**, *41*, 2132. (b) Fürstner, A.; Hannen, P. *Chem. Commun.* **2004**, 2546. (c) Böhringer, S.; Gagosz, F. *Adv. Synth. Catal.* **2008**, *350*, 2617. (d) Lim, C.; Kang, J.-E.; Lee, J.-E.; Shin, S. *Org. Lett.* **2007**, *9*, 3539. (e) Buzas, A. K.; Istrate, F. M.; Gagosz, F. *Angew. Chem., Int. Ed.* **2007**, *46*, 1141. (f) Solorio, C. R.; Echavarren, A. M. *J. Am. Chem. Soc.* **2010**, *132*, 11881.
(7) Jiménez-Núñez, E.; Raducan, M.; Lauterbach, T.; Molawi, K.; Solorio, C. R.; Echavarren, A. M. *Angew. Chem., Int. Ed.* **2009**, *48*, 6152.
(8) (a) Li, J.; Liu, X.; Lee, D. *Org. Lett.* **2012**, *14*, 410. (b) Wang, S.; Zhang, L. *J. Am. Chem. Soc.* **2006**, *128*, 14274.
(9) Kirsch, S. F.; Binder, J. T.; Crone, B.; Duschek, A.; Haug, T. T.; Liébert, C.; Menz, H. *Angew. Chem., Int. Ed.* **2007**, *46*, 2310.
(10) Bae, H. J.; Baskar, B.; An, S. E.; Cheong, J. Y.; Thangadurai, D. T.; Hwang, I.-C.; Rhee, Y. H. *Angew. Chem., Int. Ed.* **2008**, *47*, 2263.
(11) (a) Zhang, L.; Kozmin, S. A. *J. Am. Chem. Soc.* **2004**, *126*, 11806. (b) Sun, J.; Conley, M.; Zhang, L.; Kozmin, S. A. *J. Am. Chem. Soc.* **2006**, *128*, 9705.
(12) Soriano, E.; Marco-Contelles, J. *Acc. Chem. Res.* **2009**, 1026.
(13) For recent theoretical studies of gold(I)-catalyzed cycloisomerizations of 1,5-enynes, see: (a) Liu, Y.; Zhang, D.; Zhou, J.; Liu, C. *J. Phys. Chem. A* **2010**, *114*, 6164. (b) Liu, Y.; Zhang, D.; Bi, S. *J. Phys. Chem. A* **2010**, *114*, 12893. (c) Fan, T.; Chen, X.; Sun, J.; Lin, Z. *Organometallics* **2012**, *31*, 4221.
(14) A further comparison with a complexed Me-substituted substrate revealed a C1−Au distance of 2.230 Å and a C2−Au of 2.241 Å, which suggest that the hapticity of the reactant complexes is mainly governed by the donating character of the substituents, rather than the steric hindrance between the alkynyl substituent and the catalyst.
(15) Nava, P.; Hagebaum-Reignier, D.; Humbel, S. *ChemPhysChem* **2012**, *13*, 2090.
(16) (a) Harrak, Y.; Blaszykowski, C.; Bernard, M.; Cariou, K.; Mainetti, E.; Mouries, V.; Dhimane, A. L.; Fensterbank, L.; Malacria, M. *J. Am. Chem. Soc.* **2004**, *126*, 8656. For examples of the formation of bicyclo[4.1.0]heptanes from 1,6-enynes, see also: (b) Anjum, S.; Marco-Contelles, J. *Tetrahedron* **2005**, *61*, 4793. (c) Nieto-Oberhuber, C.; Muñoz, M. P.; Buñuel, E.; Nevado, C.; Cárdenas, D. J.; Echavarren, A. M. *Angew. Chem., Int. Ed.* **2004**, *43*, 2402.
(17) (a) Liu, L.-P.; Hammond, G. B. *Chem. Soc. Rev.* **2012**, *41*, 3129. (b) Hashmi, A. S. K. *Angew. Chem., Int. Ed.* **2010**, *49*, 5232. (c) Fedorov, A.; Moret, M.-E.; Chen, P. *J. Am. Chem. Soc.* **2008**, *130*, 8880.
(18) (a) Hashmi, A. S. K. *Angew. Chem., Int. Ed.* **2008**, *47*, 6754. (b) López-Carrillo, V.; Huguet, N.; Mosquera, A.; Echavarren, A. M. *Chem.—Eur. J.* **2011**, *17*, 10972.
(19) (a) Fürstner, A.; Morency, L. *Angew. Chem., Int. Ed.* **2008**, *47*, 5030. (b) Seidel, G.; Mynott, R.; Fürstner, A. *Angew. Chem., Int. Ed.* **2009**, *48*, 2510.
(20) Benítez, D.; Shapiro, N. D.; Tkachouk, E.; Wang, Y.; Goddard, W. A., III; Toste, F. D. *Nat. Chem.* **2009**, *1*, 482.
(21) (a) Schubert, U.; Ackermann, K.; Aumann, R. *Cryst. Struct. Commun.* **1982**, *11*, 591. (b) Balch, A. L.; Olmstead, M. M.; Vickery, J. C. *Inorg. Chem.* **1999**, *38*, 3494.
(22) (a) Mean of 1.979(14) Å for [AuCl(NHC)] complexes (over 52 entries in the CSD, version 5.32). (b) Lin, J. C. Y.; Huang, R. T. W.; Lee, C. S.; Bhattacharyya, A.; Hwang, W. S.; Lin, I. J. B. *Chem. Rev.* **2009**, *109*, 3561. (c) Marek, P.; Loos, A.; Ferreira, M. J.; Serra, D.; Vinokurov, N.; Rominger, F.; Jäkel, C.; Hashmi, A. S. K.; Limbach, M. *Organometallics* **2010**, *20*, 4448.
(23) (a) DeKock, R. L.; Baerends, E. J.; Boerrigter, P. M.; Hengelmolen, R. *J. Am. Chem. Soc.* **1984**, *106*, 3387. (b) Schwerdtfeger, P.; Hermann, H. L.; Schmidbaur, H. *Inorg. Chem.* **2003**, *42*, 1334. (c) David, V.; Partyka, J. B.; Updegraff, M. Z.; Hunter, A. D.; Gray, T. G. *Organometallics* **2009**, *28*, 1666. (d) Döpp, R.; Lothschütz, C.; Wurm, T.; Pernpointner, M.; Keller, S.; Rominger, F.; Hashmi, A. S. K. *Organometallics* **2011**, *30*, 5894.
(24) Fedorov, A.; Couzijn, E. P. A.; Nagornova, N. S.; Boyarkin, O. V.; Rizzo, T. R.; Chen, P. *J. Am. Chem. Soc.* **2010**, *132*, 13789.
(25) This interaction involves a high energy (793.1 kcal/mol), whereas the breaking C1−C6 bond shows a weaker interaction (217.4 kcal/mol).
(26) Benítez, D.; Tkatchouk, E.; Gonzalez, A. Z; Goddard, W. A.; Toste, F. D. *Org. Lett.* **2009**, *11*, 4798.
(27) Similar effects have been calculated for transition states for 1,2-H shifts of singlet carbenes. See: (a) Keating, A. E.; García-Garibay, M. A.; Houk, K. N. *J. Phys. Chem. A* **1998**, *102*, 8467. and references therein. (b) Albu, T. V.; Lynch, B. J.; Truhlar, D. G.; Goren, A. C.; Hrovat, D. A.; Borden, W. T.; Moss, R. A. *J. Phys. Chem. A* **2002**, *106*, 5323.
(28) Frisch, M. J.; Trucks, G. W.; Schlegel, H. B.; Scuseria, G. E.; Robb, M. A.; Cheeseman, J. R.; Montgomery, J. A., Jr.; Vreven, T.; Kudin, K. N.; Burant, J. C.; Millam, J. M.; Iyengar, S. S.; Tomasi, J.; Barone, V.; Mennucci, B.; Cossi, M.; Scalmani, G.; Rega, N.; Petersson, G. A.; Nakatsuji, H.; Hada, M.; Ehara, M.; Toyota, K.; Fukuda, R.; Hasegawa, J.; Ishida, M.; Nakajima, T.; Honda, Y.; Kitao, O.; Nakai, H.; Klene, M.; Li, X.; Knox, J. E.; Hratchian, H. P.; Cross, J. B.; Bakken, V.; Adamo, C.; Jaramillo, J.; Gomperts, R.; Stratmann, R. E.; Yazyev, O.; Austin, A. J.; Cammi, R.; Pomelli, C.; Ochterski, J. W.; Ayala, P. Y.; Morokuma, K.; Voth, G. A.; Salvador, P.; Dannenberg, J. J.; Zakrzewski, V. G.; Dapprich, S.; Daniels, A. D.; Strain, M. C.; Farkas, O.; Malick, D. K.; Rabuck, A. D.; Raghavachari, K.; Foresman, J. B.; Ortiz, J. V.; Cui, Q.; Baboul, A. G.; Clifford, S.; Cioslowski, J.; Stefanov, B. B.; Liu, G.; Liashenko, A.; Piskorz, P.; Komaromi, I.; Martin, R. L.; Fox, D. J.; Keith, T.; Al-Laham, M. A.; Peng, C. Y.; Nanayakkara, A.; Challacombe, M.; Gill, P. M. W.; Johnson, B.; Chen, W.; Wong, M. W.; Gonzalez, C.; Pople, J. A. *Gaussian 03*, revision C.02; Gaussian, Inc.: Wallingford, CT, 2004.
(29) Frisch, M. J.; Trucks, G. W.; Schlegel, H. B.; Scuseria, G. E.; Robb, M. A.; Cheeseman, J. R.; Scalmani, G.; Barone, V.; Mennucci, B.; Petersson, G. A.; Nakatsuji, H.; Caricato, M.; Li, X.; Hratchian, H. P.; Izmaylov, A. F.; Bloino, J.; Zheng, G.; Sonnenberg, J. L.; Hada, M.; Ehara, M.; Toyota, K.; Fukuda, R.; Hasegawa, J.; Ishida, M.; Nakajima, T.; Honda, Y.; Kitao, O.; Nakai, H.; Vreven, T.; Montgomery, J. A., Jr.; Peralta, J. E.; Ogliaro, F.; Bearpark, M.; Heyd, J. J.; Brothers, E.; Kudin, K. N.; Staroverov, V. N.; Kobayashi, R.; Normand, J.; Raghavachari, K.; Rendell, A.; Burant, J. C.; Iyengar, S. S.; Tomasi, J.; Cossi, M.; Rega, N.; Millam, J. M.; Klene, M.; Knox, J. E.; Cross, J. B.; Bakken, V.; Adamo, C.; Jaramillo, J.; Gomperts, R.; Stratmann, R. E.; Yazyev, O.; Austin, A. J.; Cammi, R.; Pomelli, C.; Ochterski, J. W.; Martin, R. L.; Morokuma, K.; Zakrzewski, V. G.; Voth, G. A.; Salvador, P.; Dannenberg, J. J.; Dapprich, S.; Daniels, A. D.; Farkas, O.; Foresman, J. B.; Ortiz, J. V.; Cioslowski, J.; Fox, D. J. *Gaussian09*, revision A.02; Gaussian, Inc.: Wallingford, CT, 2009.
(30) (a) Becke, A. D. *J. Chem. Phys.* **1993**, *98*, 5648−5652. (b) Lee, C.; Yang, W.; Parr, R. G. *Phys. Rev. B* **1988**, *37*, 785−789.
(31) Hay, P. J.; Wadt, W. R. *J. Chem. Phys.* **1985**, *82*, 270−283.
(32) Gonzalez, C.; Schlegel, H. B. *J. Phys. Chem.* **1990**, *94*, 5523−5527.

(33) (a) Zhao, Y.; Truhlar, D. G. *Acc. Chem. Res.* **2008**, *41*, 157−167. (b) Zhao, Y.; Truhlar, D. G. *Theor. Chem. Acc.* **2008**, *120*, 215−241.
(34) Faza, O. N.; Alvarez-Rodríguez, R.; Silva-Lopez, C. *Theor. Chem. Acc.* **2011**, *128*, 647−661.
(35) (a) Tomasi, J.; Persico, M. *Chem. Rev.* **1994**, *94*, 2027−2094. (b) Tomasi, J.; Mennucci, B.; Cammi, R. *Chem. Rev.* **2005**, *105*, 2999−3094.